ISET Journal of Earthquake Technology, Paper No. 473, Vol. 43, No. 4, December 2006, pp. 105-120

LIQUEFACTION MITIGATION OF GROUND TREATED WITH GRANULAR PILES: DENSIFICATION EFFECT

A. Murali Krishna*, M.R. Madhav** and G. Madhavi Latha*

*Department of Civil Engineering
Indian Institute of Science, Bangalore-560012
**Department of Civil Engineering
Jawaharlal Nehru Technological University, Hyderabad-500072

ABSTRACT

Ground treatment by rammed granular piles can offer effective solution amongst various other improvement methods. Densification of the surrounding ground by rammed granular piles modifies the soil properties. In this paper liquefaction mitigation of the ground treated by granular piles (GPs) is assessed considering the pore pressure generation and dissipation accounting for both the densification and drainage effects of GPs. Seed and Booker's approach for pore water pressure generation and dissipation is applied with modifications for evaluating the densification effect of GPs. Specifically the modifications in coefficients of volume change and permeability of the soil surrounding the granular drains due to the densification effect are incorporated in the analysis under earthquake conditions and their effects quantified.

KEYWORDS: Ground Improvement, Granular Piles, Densification, Pore Pressure, Earthquake

INTRODUCTION

Deposits of loose granular soils get affected by ground vibrations induced by earthquakes or cyclic loading, resulting in large total and differential settlements of the ground. Saturated granular material, when subjected to cyclic loading involving the reversal of shear stress, tends to compact or densify. In cases where the soil consists of loose granular materials and high water table, the tendency to get densified may result in the development of excess hydrostatic pore water pressures of sufficient magnitude to cause liquefaction of the soil, thus resulting in settlements and tilting of structures. A qualitative understanding of the mechanism underlying the liquefaction of saturated sands subjected to cyclic loading, such as that induced by earthquakes, had been recognized widely since being first examined by Casagrande in 1936 (Martin et al., 1975). For a saturated sand under undrained conditions, the tendency for volume reduction during each cycle of loading results in a corresponding progressive increase in pore-water pressure. If the magnitude of pore-water pressure generated equals the confining pressure, the effective stress becomes zero and the soil is said to have liquefied. Pore pressure buildup leading to liquefaction may be due to static or cyclic stress applications and the possibility of its occurrence depends on the void ratio or relative density of sand and the confining pressure (Seed, 1979). A possible method of stabilizing a soil deposit susceptible to liquefaction is to install a system of gravel or rock drains (Seed and Booker, 1977).

It is observed that granular piles are effective in mitigating liquefaction damage due to the reinforcement effect and drainage facility. Adalier and Elgamal (2004) reviewed the current state of the stone column technologies as a liquefaction countermeasure. Due to the installation of gravel drains, the generated pore water pressure due to repeated loading may get dissipated almost as fast as it is generated. In addition to these reinforcement and drainage effects, densification of the ambient soil around the rammed granular pile (RGP) should also be considered for total and better evaluation of improvement. Granular piles are of the displacement type and hence densify in-situ ground during the process of installation (Madhav, 2001). The effect of densification is manifested through an increase in the coefficient of earth pressure at rest (Massarsch and Fellenius, 2002) and in the value of modulus of deformation of the soil (Ohbayashi et al., 1999). Ohbayashi et al. (1999) summarized measured values of Swedish Weight Sounding, (N_{sw}), SPT N and CPT (q_c) at different sites wherein the increase in the measured parameters is presented as a function of the distance from the center of the compaction point. The densification effect becomes negligible at a distance of about 2.0 m from the center of the sand

compaction piles (SCPs) but the increase depends on the fines content (Figure 1). Densification by RGP causes increase in deformation moduli and decrease in the coefficients of permeability and volume change. Further, the densification effect decreases with distance from the center of the compaction point and may become negligible at the periphery of unit cell. Thus, the coefficients of horizontal permeability, $k_h(r)$, and volume change, $m_v(r)$, of the soil around the granular pile can be considered to vary with distance r from the center of the pile.

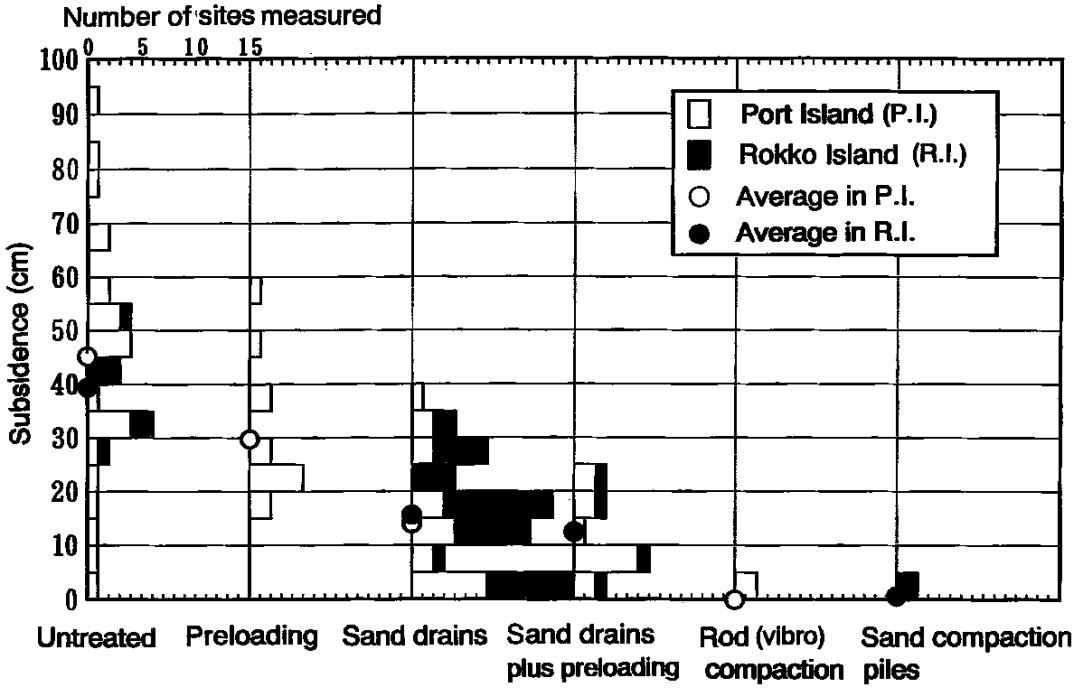

Fig. 2 Comparison of ground subsidence in zones treated with different methods (after Yasuda et al., 1996)

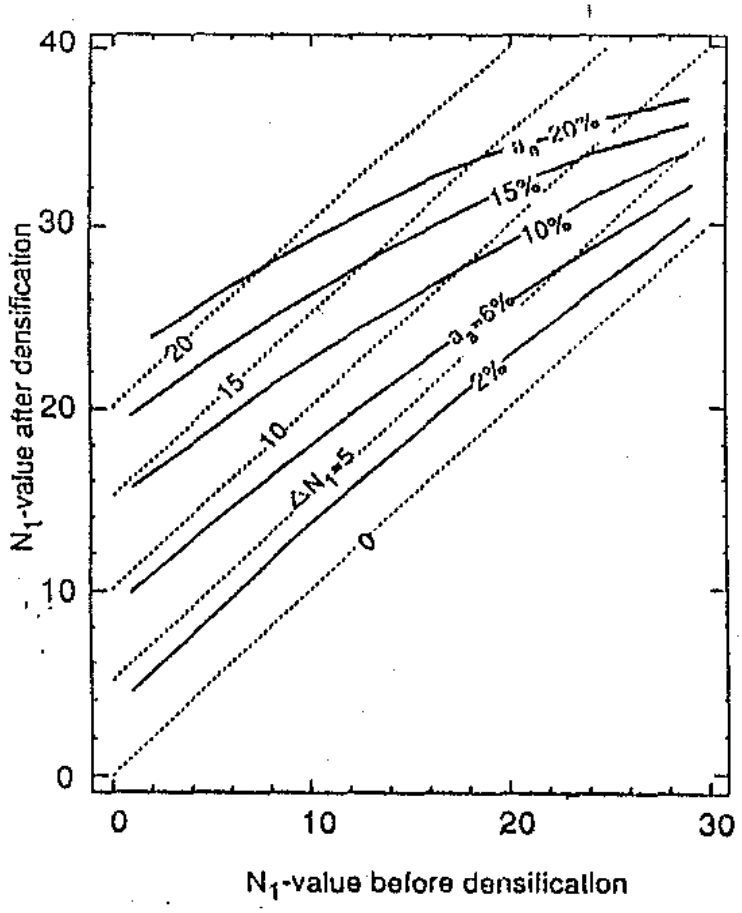

Fig. 3 Diagram for the evaluation of increase in SPT N_1-value (after Tsukamoto et al., 2000)

Densification and reinforcement effects cause modifications in the properties of the in-situ soil. This densification and modification in the soil parameters of the ground is not uniform over the entire zone of surrounding ground and is function of the distance from the point of densification. During the process of

installation of RGPs, the soil adjacent to and in the vicinity of the point of treatment gets densified most. Thus, the densification effect of the ground, due to the installation of a granular pile, is maximum near the periphery of the pile and decreases with the distance from the pile. Densification by RGPs causes increase in the deformation moduli and decrease in the coefficient of permeability and coefficient of volume change.

Sujatha (1998) analyzed several field-test data and postulated linear and exponential variations of the stiffness of soil with distance as limits for the densification effect. Similar variations are considered for the reduction of flow and deformation parameters of the in-situ soil (i.e., coefficients of permeability and volume change). This reduction is maximum at the point of densification and decays with distance towards the periphery of the unit cell, with the parameters reaching their original in-situ values at the farthest end of the unit cell.

LINEAR VARIATION OF THE FLOW PARAMETERS

As a consequence of densification, a linear variation of the coefficient of horizontal permeability, k_h, with distance from the center of RGP is considered, with k_h becoming minimum at the edge of RGP $(r = a)$ and maximum at the periphery of the unit cell $(r = b)$ (Figure 4). The expression for the coefficient of permeability at distance r from the centre of the granular pile considering linear variation is

$$k_h(r) = \left(\frac{k_{sb} - k_{sa}}{b - a}\right)(r - a) + k_{sa} \tag{1}$$

where k_{sa} and k_{sb} are the coefficients of permeability at the edges of RGP $(r = a)$ and unit cell $(r = b)$, respectively. Non-dimensionalizing Equation (1) with k_{hi}, the initial in-situ value of the coefficient of permeability, one gets

$$R_k(r) = \left(\frac{R_{kb} - R_{ka}}{b - a}\right)(r - a) + R_{ka} \tag{2}$$

where $R_k = k_h / k_{hi}$, $R_{kb} = k_{sb} / k_{hi}$, and $R_{ka} = k_{sa} / k_{hi}$.

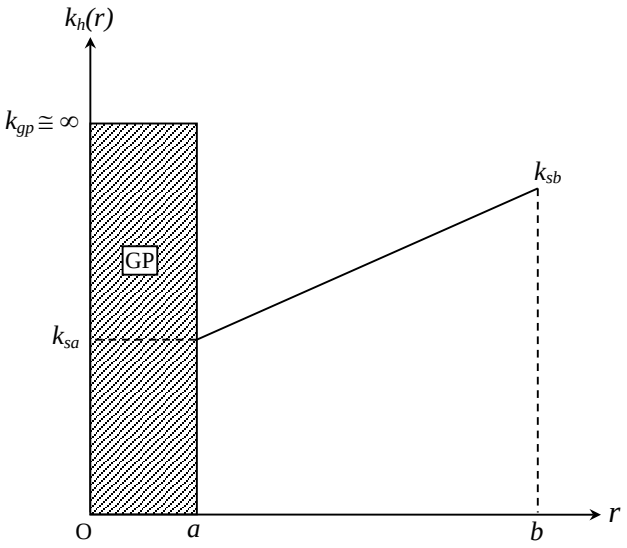

Fig. 4 Variation of coefficient of permeability of soil with distance

Similarly, the expression for linear variation of the coefficient of volume change, m_v, is

$$m_v(r) = \left(\frac{m_{vb} - m_{va}}{b - a}\right)(r - a) + m_{va} \tag{3}$$

where m_{va} and m_{vb} are, respectively, the coefficients at distances a and b from the centre. Non-dimensionalizing Equation (3) with m_{vi}, the initial in-situ value of the coefficient of volume change, one gets

$$R_{mv}(r) = \left(\frac{R_{mb} - R_{ma}}{b - a} \right)(r - a) + R_{ma} \tag{4}$$

SEED AND BOOKER (1977) METHOD

In most practical cases, the horizontal permeability of a sand deposit is much higher than its vertical permeability and the spacing between vertical drains is closer than the distance required for pore water to drain vertically towards the free surface. Furthermore, many natural deposits of sand are interspersed with narrow horizontal layers of relatively impermeable silt, which may severely inhibit vertical drainage. For these reasons the dominant mechanism in the operation of a gravel drain system is often one of pure horizontal drainage (Seed and Booker, 1977).

For flow into gravel drain, assuming pure radial flow and constant coefficients of permeability (k_h) and volume compressibility (m_v), the governing equation for the phenomenon can be written as (Seed and Booker, 1977):

$$\frac{k_h}{\gamma_w m_v}\left(\frac{1}{r}\frac{\partial u}{\partial r} + \frac{\partial^2 u}{\partial r^2} \right) = \frac{\partial u}{\partial t} - \frac{\partial u_g}{\partial N}\frac{\partial N}{\partial t} \tag{5}$$

where u is the excess pore pressure at radial distance r from the centre, t is time, γ_w is the unit weight of water, u_g is the peak excess hydrostatic pore-water pressure generated by the earthquake, N is the number of cycles, and

$$\frac{\partial u_g}{\partial N} = \frac{\sigma'_o}{\alpha \pi N_l} \frac{1}{\sin^{2\alpha\text{-}1}\left(\frac{\pi}{2} r_u\right) \cos\left(\frac{\pi}{2} r_u\right)} \tag{6}$$

In Equation (6), $r_u = u/\sigma'_o$, the pore pressure ratio; σ'_o = the initial mean bulk effective stress for axisymmetric conditions or the initial vertical effective stress for simple shear conditions; N_l is the number of cycles required to cause liquefaction; and α is an empirical constant characterizing the shape of the pore pressure generation curve and is a function of the soil properties with a typical value of 0.7. The irregular cyclic loading induced by an earthquake is converted (Seed et al., 1975) into an equivalent number, N_{eq}, of uniform cycles at an amplitude of 65% of the peak cyclic shear stress, i.e. at $\tau_{cyc} = 0.65\tau_{\max}$, occurring over time-duration t_d, and thus,

$$\frac{\partial N}{\partial t} = \frac{N_{eq}}{t_d} \tag{7}$$

1. Assumptions and Limitations

It is assumed that the flow of the pore water is governed by Darcy's law; the coefficients of permeability and compressibility remain constant; drainage or flow is horizontal; and the granular filler material is far more permeable than the surrounding sand layer.

Following are the limitations of the method by Seed and Booker (1977). Infinite gravel drain permeability is assumed so that no excess pore water pressures are developed in the columns. The smear resistance is not accounted for and so is the case with the possible clogging of the drain due to the migration of fine sediments towards the drain due to pore pressure generation. This model applies to low pore pressure ratio values where a linear process of consolidation is valid. This process assumes the coefficient of compressibility to be constant.

2. Recent Related Studies

Design diagrams by Onoue (1988) and Iai and Koizumi (1986) incorporated the effects of drain resistance in the analyses of Seed and Booker (1977). Baez and Martin (1992) presented an evaluation of the relative effectiveness of stone columns for the mitigation of liquefaction of soil. Pestana et al. (1998) analysed the development of excess pore pressure in a layered soil profile, accounting for vertical and horizontal drainage with a non-constant 'equivalent hydraulic conductivity', and head losses due to horizontal flow into the drain and also the presence of a reservoir directly connected to the drain were considered. Boulanger et al. (1998) evaluated the drainage capacity of stone columns or gravel drains for mitigating liquefaction hazards.

NEW MODEL CONSIDERING DENSIFICATION OF GROUND

The governing equation of the model by Seed and Booker (1977) (Equation (5)) is modified to include the densification effect of RGP in dissipating the excess pore-water pressure. In the ground treated with RGP, coefficient of permeability (k_h) and coefficient of volume compressibility (m_v) are considered to depend on the distance r, instead of being constant values.

Consider an element of soil, in polar coordinates as shown in Figure 5, through which laminar flow occurs. Using Darcy's law, from the expression for the flow in the radial direction, the basic flow equation is obtained as

$$\frac{k_h(r)}{r}\frac{\partial h}{\partial r}+k_h(r)\frac{\partial^2 h}{\partial r^2}+\frac{\partial k_h(r)}{\partial r}\frac{\partial h}{\partial r}=\frac{S}{1+e}\frac{\partial e}{\partial t} \tag{8}$$

Using the stress-strain relations and definitions of coefficient of compressibility (a_v) and coefficient of volume change (m_v), it is possible to write for $S=1$ (fully-saturated case),

$$\frac{1}{1+e}\frac{\partial e}{\partial t}=m_v\left(\frac{\partial u}{\partial t}-\frac{\partial \sigma}{\partial t}\right) \tag{9}$$

From Equation (9) and with $h=u/\gamma_w$ (u = excess pore pressure, γ_w = unit weight of water), Equation (8) is rewritten as

$$\frac{k_h(r)}{\gamma_w m_v(r)}\left(\frac{1}{r}\frac{\partial u}{\partial r}+\frac{\partial^2 u}{\partial r^2}\right)+\frac{1}{\gamma_w m_v(r)}\frac{\partial(k_h(r))}{\partial r}\frac{\partial u}{\partial r}=\frac{\partial u}{\partial t}-\frac{\partial \sigma}{\partial t} \tag{10}$$

where $k_h(r)$ and $m_v(r)$ are as defined in Equations (1) and (3) respectively. Considering the rate of change of total stress, $\frac{\partial \sigma}{\partial t}$, as the rate of pore pressure generation, one may write

$$\frac{\partial u_g}{\partial t}=\frac{\partial u_g}{\partial N}\frac{\partial N}{\partial t} \tag{11}$$

The final form of Equation (10) therefore becomes,

$$\frac{k_h(r)}{\gamma_w m_v(r)}\left(\frac{1}{r}\frac{\partial u}{\partial r}+\frac{\partial^2 u}{\partial r^2}\right)+\frac{1}{\gamma_w m_v(r)}\frac{\partial(k_h(r))}{\partial r}\frac{\partial u}{\partial r}=\frac{\partial u}{\partial t}-\frac{\partial u_g}{\partial N}\frac{\partial N}{\partial t} \tag{12}$$

Equation (12) is a more generalized equation considering all forms of non-homogeneity. In non-dimensional form, with normalized pore pressure $W=u/\sigma_o'$, which is same as the pore pressure ratio r_u (Seed and Booker, 1977), and with $W_g=u_g/\sigma_o'$, Equation (12) becomes

$$\frac{k_h(r)}{\gamma_w m_v(r)}\left(\frac{1}{r}\frac{\partial W}{\partial r}+\frac{\partial^2 W}{\partial r^2}\right)+\frac{1}{\gamma_w m_v(r)}\frac{\partial(k_h(r))}{\partial r}\frac{\partial W}{\partial r}=\frac{\partial W}{\partial t}-\frac{\partial W_g}{\partial N}\frac{\partial N}{\partial t} \tag{13}$$

Non-dimensionalising the terms r and t via $R\ (=r/b)$ and $T\ (=t/t_d)$ respectively, Equation (13) becomes

$$T_{bd}\frac{R_k(R)}{R_{mv}(R)}\left(\frac{\partial^2 W}{\partial R^2}+\frac{1}{R}\frac{\partial W}{\partial R}\right)+\frac{T_{bd}}{R_{mv}(R)}\frac{\partial R_k(R)}{\partial R}\frac{\partial W}{\partial R}=\frac{\partial W}{\partial T}-\frac{\partial W_g}{\partial N}N_{eq} \tag{14}$$

where

$$\frac{\partial W_g}{\partial N}=\frac{1}{\alpha\pi N_l}\frac{1}{\sin^{2\alpha-1}\left(\frac{\pi}{2}r_u\right)\cos\left(\frac{\pi}{2}r_u\right)} \tag{15}$$

and

$$T_{bd}=\left(\frac{k_{hi}}{\gamma_w}\frac{t_d}{m_{vi}}\right)\frac{1}{b^2} \tag{16}$$

Equation (14) is nonlinear and hence is solved numerically using a finite-difference approach, which involves discretizing the unit cell radially into a number of elements, for the appropriate boundary and initial conditions (Murali Krishna, 2003).

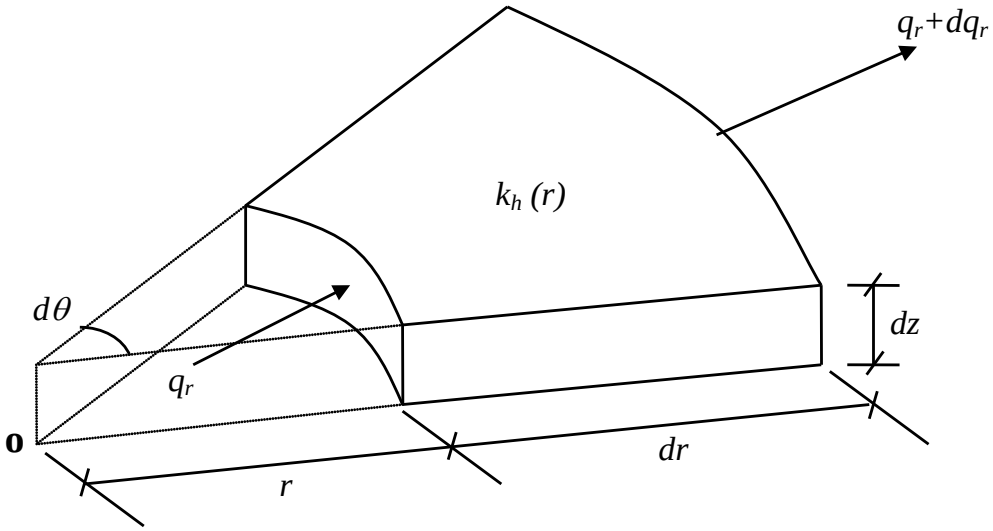

Fig. 5 Flow through a soil element

1. Boundary Conditions

The material in the drain is far more permeable than the surrounding sand layer. So the excess pore-water pressure in the drain is effectively zero, i.e., at $r=a$ or $R=a/b$, $u=0$ or $W=0$ (Gravel drain is infinitely permeable). At the outer boundary of the unit cell, due to symmetry, the pore-water pressure dissipation in the radial direction is zero, i.e., at $r=b$ or $R=1$,

$$\frac{\partial u}{\partial r}=0 \quad \text{or} \quad \frac{\partial W}{\partial R}=0 \tag{17}$$

2. Initial Condition

At $t=0$ or $T=0$, pore pressure at all the nodes in the soil is equal to the average of pore water pressure generated over the initial time period of dt (or dT), i.e., average of the pore-water pressure generated over the initial cycle dN. Therefore,

$$W_g\big|_{\text{at } T=0}=\frac{u_g}{\sigma'_o}\bigg|_{\text{at } t=0}=\frac{1}{2}\left(\frac{2}{\pi}\arcsin\left(\frac{dN}{N_l}\right)^{1/2\alpha}\right) \tag{18}$$

3. Limitations

The assumptions and limitations associated with the original model of Seed and Booker (1977) are carried to the new model also. The smear effect is commonly included through a reduction in the permeability. However, the limitations due to the assumption of infinite permeability for the drain and neglect of the possible clogging of the drain with sediments still remain.

RESULTS AND DISCUSSION

Under the assumption of purely radial flow, the pore pressure ratio, $W = u/\sigma'_o$, throughout the sand depends on the dimensionless parameters: a/b = ratio representing the geometric configuration of the RGP; N_{eq}/N_l = cyclic ratio characterizing the severity of the earthquake shaking, in relation to the liquefaction characteristics of the sand; T_{bd} , relating the duration of the earthquake to the consolidation properties of the sand; α , a parameter characterizing the shape of the pore pressure generation curve. It is found that for many materials, $\alpha = 0.7$ fits the experimental data well, and this value is adopted (Seed et al. 1976), with $R_k(r)$ and $R_{mv}(r)$ (or $R_k(R)$ and $R_{mv}(R)$) that are functions of radial distance r, defining the variations of coefficient of horizontal permeability and volume compressibility of soil, respectively.

1. 'No Densification' Case for Validation

If the coefficients of permeability and volume change of the surrounding soil are unchanged due to the installation of RGP, this represents the 'No Densification' case. In this case the ambient soil will have the initial values of k_{hi} and m_{vi} (i.e., $R_{ka} = R_{kb} = R_{ma} = R_{mb} = 1$). This condition of 'No Densification' is identical to the solution of Seed and Booker (1977). The effect of a/b ratio on maximum pore water pressure in the present study is shown in Figure 6 for the cyclic ratio (N_{eq}/N_l) of 2 and a range of a/b (0.1 to 0.4), with T_{bd} = 1, along with the results obtained by Seed and Booker (1977) for the similar conditions but by using the finite element program LARF (Liquefaction Analysis for Radial Flow). Maximum pore pressure ratio $W_{\max}(T)$, i.e. the maximum value of u/σ'_o , throughout the layer is plotted against $T\,(t/t_d)$. This figure provides a comparison between the solutions of the finite element method of Seed and Booker (1977) and the present finite-difference method. The results obtained in the present study agree closely with the results of Seed and Booker (1977). Small deviations discernible between the two solutions may be due to the method of solution and due to the time-step involved. Moreover, it is observed that the deviations decrease with an increase in the area ratio. For the cyclic ratio (N_{eq}/N_l) equal to 2, if no drains are present $(a/b = 0)$, the soil liquefies at $T_l = 1/(N_{eq}/N_l)$, i.e., at $T = 0.5$. It is observed from the figure that, for $a/b = 0.1$, initial liquefaction is deferred for a period of T but eventually occurs at about $T = 0.6$. The liquefied state, $W_{\max} = 1$, continues until the end of the period of strong shaking. Thereafter it decreases as pore-water pressure dissipates. It can be observed that at higher a/b values, initial liquefaction may be prevented as the maximum pore pressure ratio decreases with an increase in the a/b ratio.

Effect of cyclic ratio on the maximum pore pressure ratio, without densification effect, is shown in Figure 7. A range of cyclic ratio, N_{eq}/N_l , from 1 to 5 with a/b = 0.3 and T_{bd} = 1 is considered. As cyclic ratio increases, pore water pressure increases and leads to liquefaction depending on the generation and dissipation of pore pressures. The time at which the ground liquefies decreases with an increase in the cyclic ratio as per $T_l = 1/(N_{eq}/N_l)$. If attained, the liquefied state continues until the end of the period of strong shaking, i.e., $T = 1$. Thereafter, the pore pressure ratio decreases gradually. It can be observed from Figure 7 that the peak value of $W_{\max}$ increases from about 0.27 to 0.52 for an increase in N_{eq}/N_l

from 1 to 2. For the N_{eq}/N_l values of 3, 4 and 5, $W_{\max}$ reaches a value of unity at the T values of about 0.62, 0.35 and 0.24, respectively.

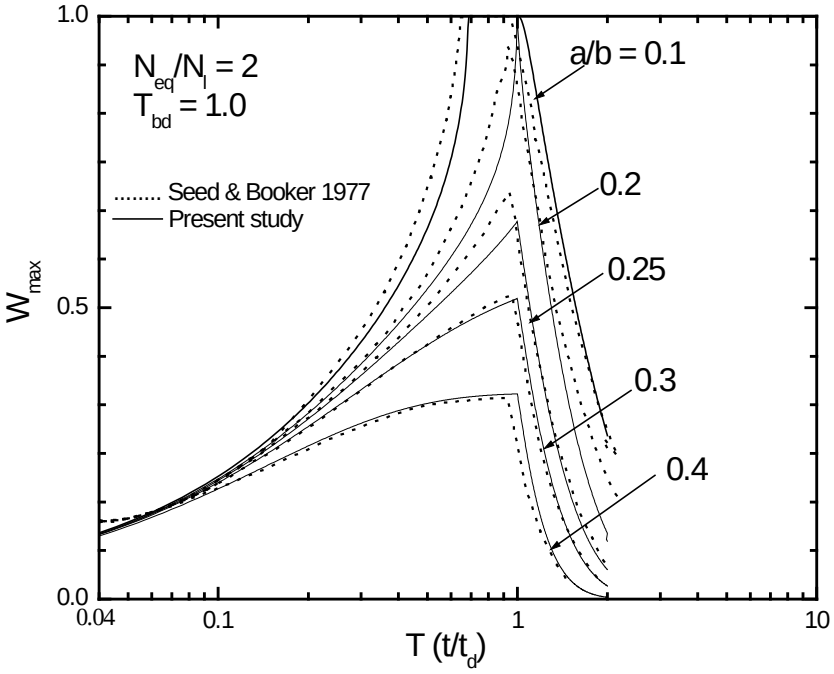

Fig. 6 Effect of the area ratio on $W_{\max}$ for the 'No Densification' case

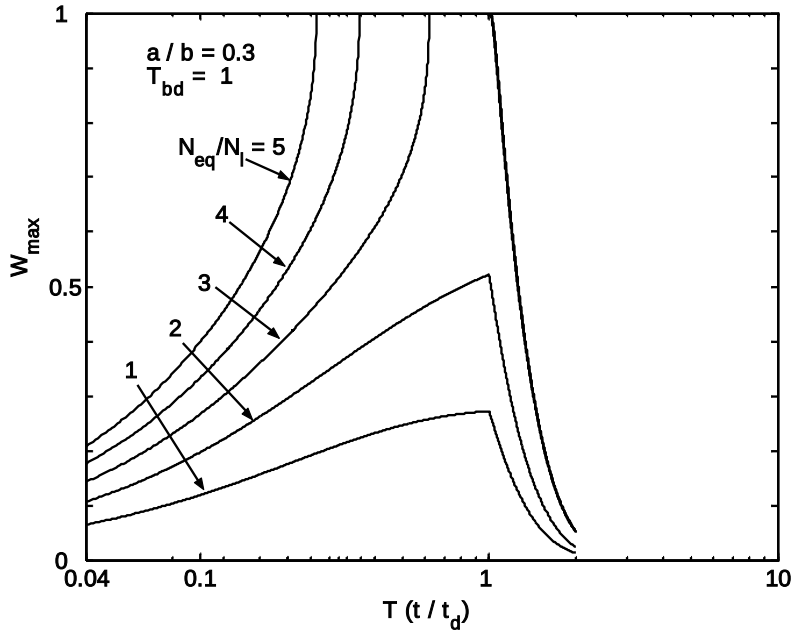

Fig. 7 Effect of the N_{eq}/N_l ratio on $W_{\max}$ for the 'No Densification' case

2. Densification Case

Densification effect on the maximum pore pressure ratio $W_{\max}$ with respect to change only in the coefficient of volume change (i.e., no change in the coefficient of permeability $(R_{ka} = R_{kb} = 1)$) is shown in Figures 8 and 9. Figure 8 shows the effect of densification at the near end, R_{ma}, on $W_{\max}$, for no modification in the coefficient of volume change at the farthest end $(R_{mb} = 1)$. A range of R_{ma} from

0.1 to 1 is considered with $T_{bd}=1$, $a/b=0.3$ and $N_{eq}/N_l=2$. It can be observed that the maximum pore pressure ratio $W_{\max}$ decreases with decrease in R_{ma}; it decreases from 0.525 to 0.375 for a decrease in R_{ma} from 1 to 0.1. The effect of densification at the farthest end (R_{mb}) is shown in Figure 9, considering densification at the near end, R_{ma}, as 0.3. A range of R_{mb} from 0.5 to 1 is considered with $T_{bd}=1$, $a/b=0.3$ and $N_{eq}/N_l=2$. It can be observed that $W_{\max}$ decreases from 0.41 to 0.25 for a decrease in R_{mb} from 1 to 0.5. It can be concluded from Figures 8 and 9 that densification effects with respect to the coefficient of volume change reduce the pore pressures and mitigate the liquefaction potential.

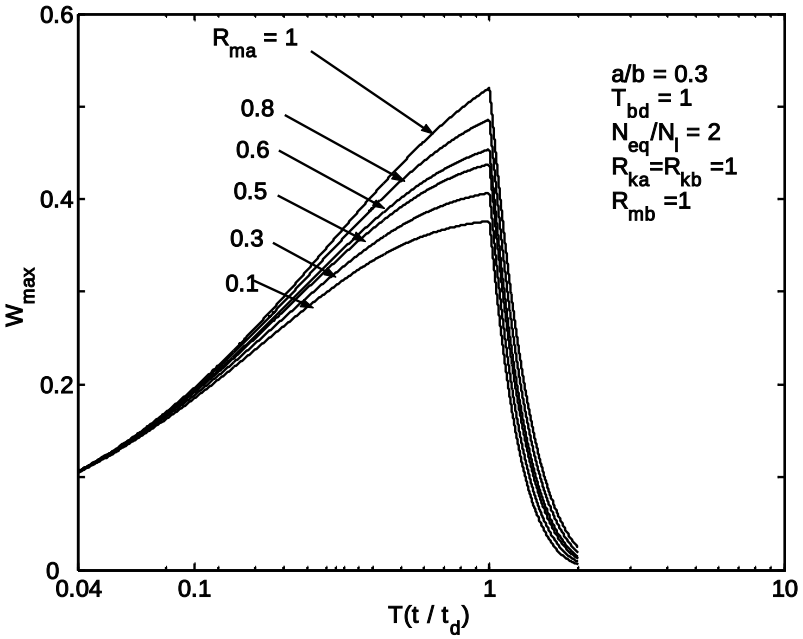

Fig. 8 Densification effect with respect to the compressibility coefficient at the near end on $W_{\max}$

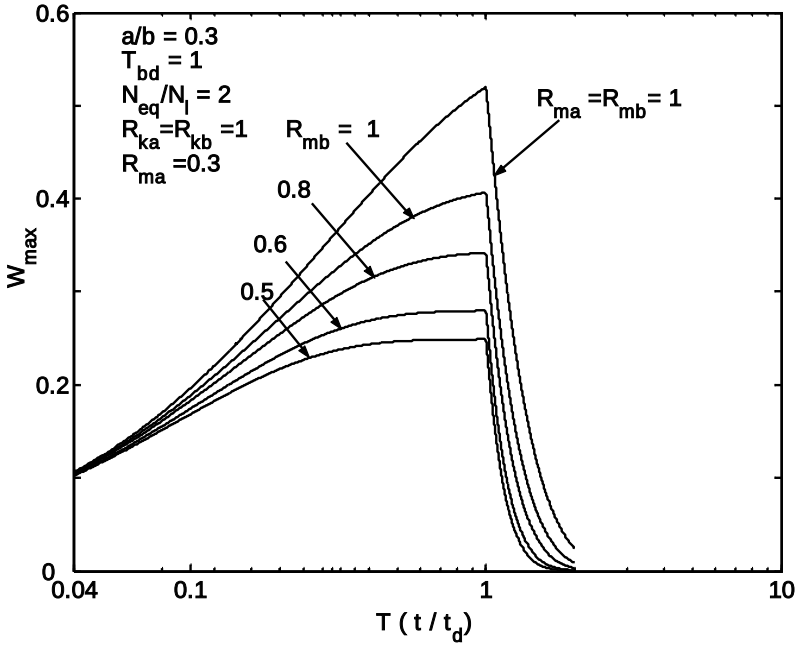

Fig. 9 Densification effect with respect to the compressibility coefficient at the farthest end on $W_{\max}$

Densification effect on the maximum pore pressure ratio in terms of change only in the coefficient of permeability, i.e., no change in the coefficient of volume change $(R_{ma} = R_{mb} = 1)$, is shown in Figures 10 and 11. The effect of densification at the near end, R_{ka}, on $W_{\max}$, for no modification in the coefficient of permeability at the farthest end $(R_{kb} = 1)$, is shown in Figure 10. A range of R_{ka} from 0.5 to 1 is considered with $T_{bd} = 1$, $a/b = 0.3$ and $N_{eq}/N_l = 2$. It may be observed that $W_{\max}$ increases from 0.525 to 0.675 for a decrease in R_{ka} from 1 to 0.8. For $R_{ka} = 0.6$ the maximum pore pressure ratio reaches unity, which corresponds to the liquefied state. Further decrease in R_{ka} will reduce the time to attain the liquefied state. The effect of densification at the farthest end (R_{kb}) on the maximum pore pressure ratio is shown in Figure 11, considering densification at the near end, R_{ka}, as 0.6. A range of R_{kb} from 0.6 to 1 is considered with $T_{bd} = 1$, $a/b = 0.3$ and $N_{eq}/N_l = 2$. It can be observed that the maximum pore pressure ratio is slightly affected by densification at the farthest end, R_{kb}. It can be concluded from Figures 10 and 11 that densification effect with respect to the coefficient of permeability increases the pore pressures. This observation is revealing in that densification with respect to the coefficient of permeability alone results in a negative effect.

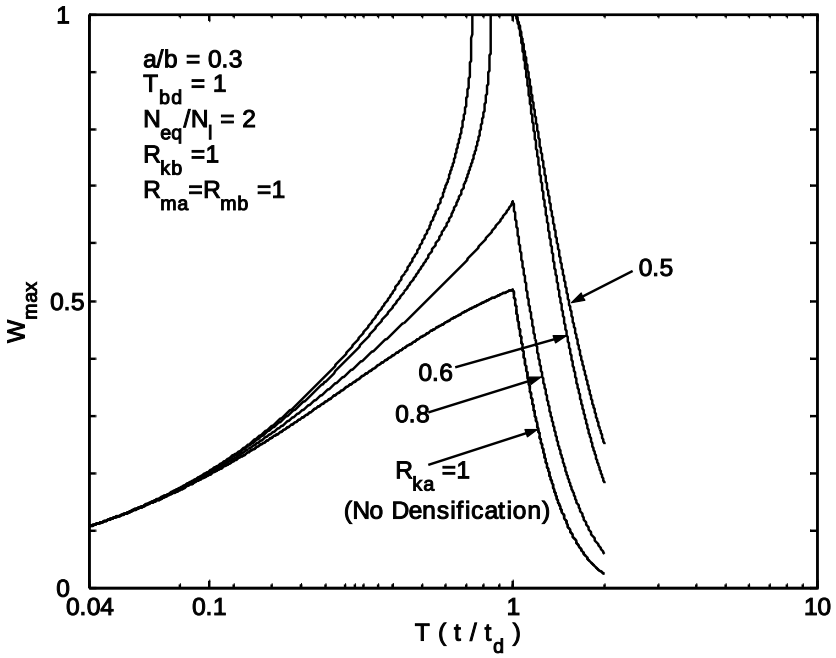

Fig. 10 Densification effect with respect to the permeability coefficient at the near end on $W_{\max}$

Figure 12 shows the densification effect on the maximum pore pressure ratio $W_{\max}$ with respect to both the coefficients of permeability and volume change at the near end. In this case the coefficients of permeability and volume change at the farthest end remain unaffected $(R_{kb} = R_{mb} = 1)$. A range of R_{ka} and R_{ma} from 0.3 to 1 is considered with $T_{bd} = 1$, $a/b = 0.3$ and $N_{eq}/N_l = 2$. Equal densification effect is considered for both R_{ka} and R_{ma}. It may be observed that the maximum pore pressure ratio increases from 0.525 to 0.62 for a decrease in R_{ka} and R_{ma} from 1 to 0.8. $W_{\max}$ becomes almost equal to 1, i.e., the ground attains liquefied state, at $T = 1$ for $R_{ka} = R_{ma} = 0.6$. Further reductions in R_{ka} and R_{ma} reduce the time *T*, corresponding to $W_{\max} = 1$.

The effect of densification at the farthest end, with respect to both coefficients of permeability (R_{kb}) and volume change (R_{mb}), on the maximum pore pressure ratio $W_{\max}$ is shown in Figure 13, while

considering densification at the near end as $R_{ka} = R_{ma} = 0.6$. This is done for both R_{kb} and R_{mb} ranging between 0.7 and 1. $W_{\max}$ attains the value of unity, indicating the liquefaction state, at $T = 1$ for $R_{kb} = R_{mb} = 1$, i.e., for no densification at the farthest end. Densification at the farthest end, associated with reduction in R_{kb} and R_{mb} (from 1 to 0.7), reduces $W_{\max}$ (from about 1 to about 0.57) and thus establishes that liquefaction of ground is mitigated by overall densification of the ground.

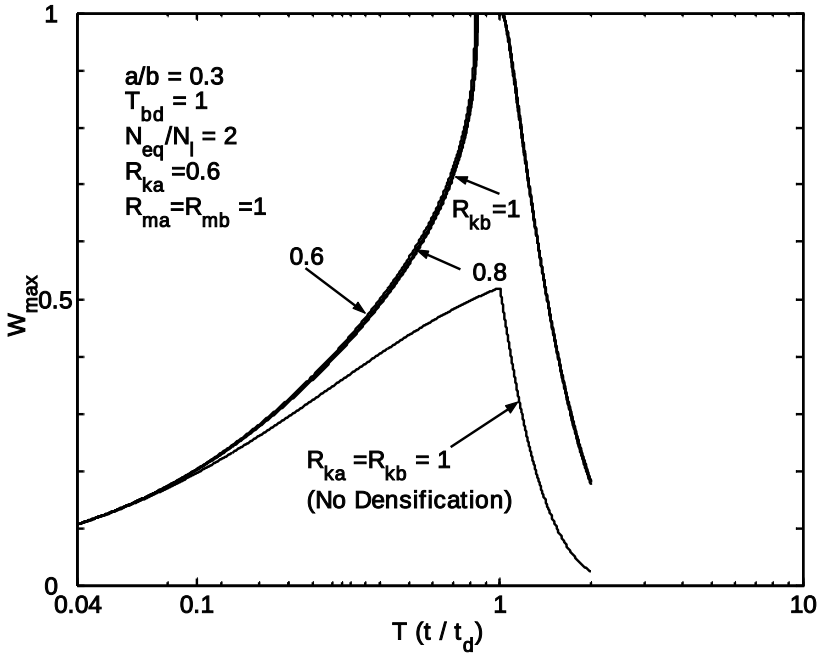

Fig. 11 Densification effect with respect to the permeability coefficient at the farthest end on $W_{\max}$

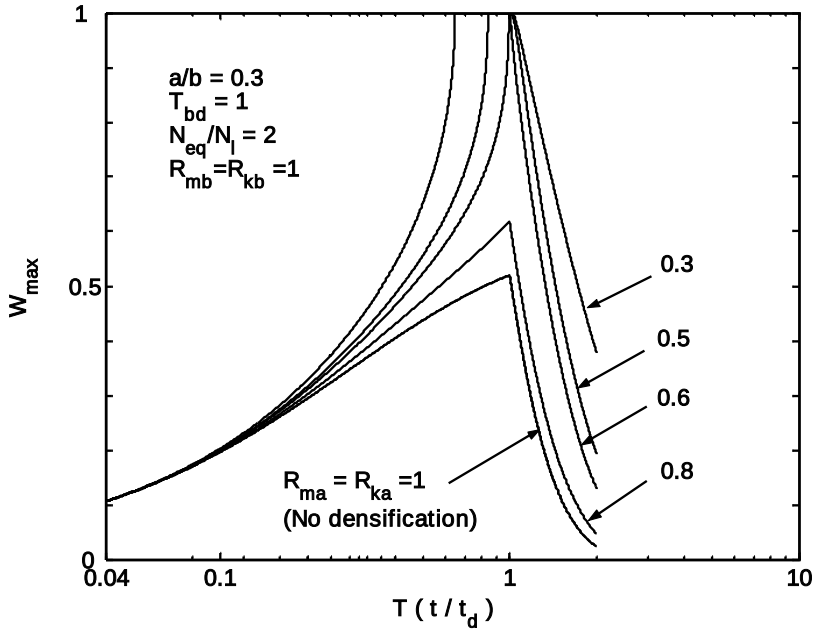

Fig. 12 Densification effect with respect to the coefficients of compressibility and permeability at the near end on $W_{\max}$

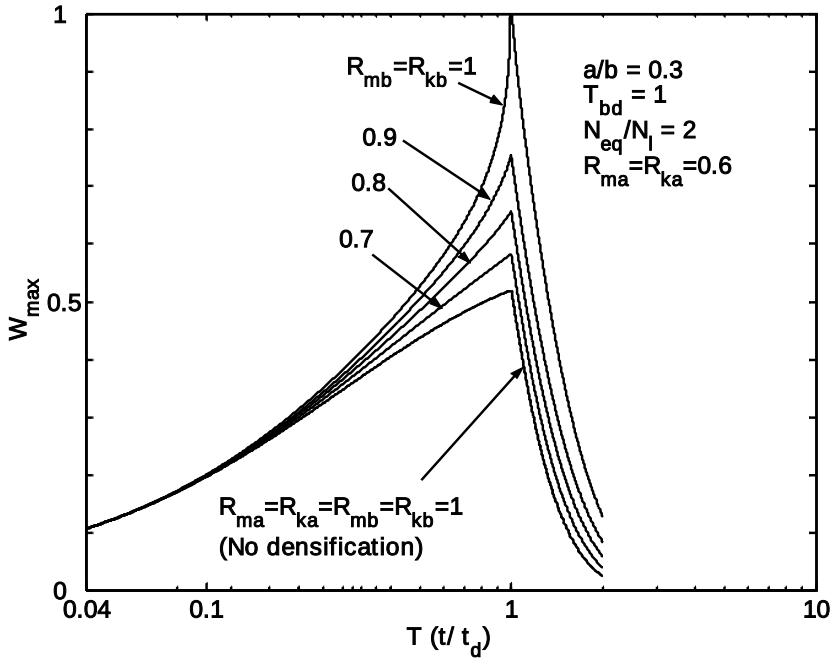

Fig. 13 Densification effect with respect to the coefficients of compressibility and permeability at the farthest end on $W_{\max}$

Practical applicability of the proposed model is illustrated by solving a typical practical situation with reasonable input parameters. Consider a soil layer having the properties, γ'_w = 9.81 kN/m^3, k_{hi} = 10^{-5} m/s and m_{vi} = 7.13×10^{-5} kN/m^2, and subjected to an earthquake ground motion that is represented by 24 uniform stress cycles in a period of 70 s. It is known that under undrained conditions (i.e., with no granular drains or RGP), the soil would liquefy under this sequence of stress application after 12 cycles so that $N_{eq}/N_l = 2$. If granular piles of 0.6 m diameter are installed at 2 m center to center spacing (a/b = 0.3, b = 1.0 m), then $T_{bd} = \left(k_{hi}t_d / \gamma_w m_{vi}\right)/b^2$ = [10^{-5}×70/(9.81×7.13×10^{-5})]/1.0^2 = 1.0.

If densification effect is not considered, the maximum pore pressure ratio generated is observed to be 0.52 (Figure 12). If densification effect is considered in terms of reductions in the values of permeability and compressibility to 0.8 times of their initial values at the periphery of the granular pile (i.e., at the near end) and no reductions at the farthest end, the maximum pore pressure ratio generated will increase to 0.62. It may also be observed from Figure 12 that if the densification effect reduces the permeability and compressibility values to 0.6 times the initial values or lower, the maximum pore pressure ratio will reach unity, thus indicating the initiation of liquefaction.

Similar mechanisms operate in the ground treated with vibrated granular piles that are installed by the vibro-replacement process. In this case the densification caused by vibration may affect the flow and compressibility parameters. Modified permeability and compressibility values should then be considered for the effective analysis of pore pressure generation and dissipation.

CONCLUSIONS

An analysis of ground treated with granular piles (stone columns), while considering the effect of installation in densifying the ground, has been proposed. Both the coefficients of volume change and permeability are considered to be affected due to densification by RGP. The reality however is that both the coefficients decrease because of densification. The densification effect decreases with the distance from the point of densification. Hence, linear variations have been adopted for the coefficients of permeability and volume change with distance. A new model has been proposed by incorporating the above variations into the classical model by Seed and Booker (1977), to include the densification effect of rammed granular piles. Pore pressure generation and dissipation in the modified ground have been studied for a range of parameters considered for the densification effect. Maximum pore pressure ratio has been

found to decrease with closer spacing of gravel drains and to increase with increase in the cyclic ratio (N_{eq}/N_l). Densification effect on the coefficient of volume change alone has been found to be positive in that the maximum induced pore pressure ratio gets reduced. Densification effect with respect to the coefficient of permeability alone increases the maximum pore water pressure ratio, thus becoming a negative effect. Densification effect with respect to both coefficients of permeability and volume change becomes a slightly negative or positive effect, depending on the relative degrees of densification with respect to compressibility and permeability. Ground treated with vibro-stone columns too would show similar effects, though the quantification of the change in the state of in-situ stress remains an intractable phenomenon to model at the present juncture.

NOTATIONS

The following symbols are used in this paper:

a	=	radius of the granular pile
b	=	radius of the unit cell
GP	=	granular pile
$k_h(r)$	=	horizontal permeability of treated ground
k_{hi}	=	horizontal permeability of untreated ground
$m_v(r)$	=	coefficient of volume compressibility of treated ground
m_{vi}	=	coefficient of volume compressibility of untreated ground
N	=	number of stress cycles associated with any period of earthquake shaking
N_{eq}	=	equivalent number of uniform stress cycles induced by earthquake
N_l	=	number of uniform stress cycles required to cause liquefaction
R	=	non-dimensionalized radial distance (= r/b)
r	=	radial distance measured from the center of granular pile
SCP	=	sand compaction pile
SPT N	=	standard penetration test number
SPT N_1	=	SPT N value corrected for the overburden stress of 100 kPa
T	=	normalized time, t/t_d
t	=	time
T_{bd}	=	dimensionless time factor
t_d	=	duration of earthquake
u	=	excess hydrostatic pressure
u_g	=	excess hydrostatic pressure generated by earthquake shaking
W or r_u	=	pore pressure ratio
$W_{\max}$	=	maximum value of pore pressure ratio W throughout the layer at a given T
σ'_o	=	initial mean bulk effective stress

REFERENCES

1. Adalier, K. and Elgamal, A. (2004). “Mitigation of Liquefaction and Associated Ground Deformations by Stone Columns”, Engineering Geology, Vol. 72, No. 3-4, pp. 275-291.

2. Baez, J.I. and Martin, G.R. (1992). "Quantitative Evaluation of Stone Column Techniques for Earthquake Liquefaction Mitigation", Proceedings of the 10th World Conference on Earthquake Engineering, Madrid, Spain, Vol. 3, pp. 1477-1483.
3. Balaam, N.P. and Booker, J.R. (1981). "Analysis of Rigid Rafts Supported by Granular Piles", International Journal for Numerical and Analytical Methods in Geomechanics, Vol. 5, No. 4, pp. 379-403.
4. Boulanger, R.W., Idriss, I.M., Stewart, D.P., Hashash, Y. and Schmidt, B. (1998). "Drainage Capacity of Stone Columns or Gravel Drains for Mitigating Liquefaction" in "Geotechnical Earthquake Engineering and Soil Dynamics III (edited by P. Dakoulas and M. Yegian)", Geotechnical Special Publication No. 75, American Society of Civil Engineers, Reston, U.S.A.
5. Datye, K.R. and Nagaraju, S.S. (1981). "Design Approach and Field Control for Stone Columns", Proceedings of the 10th International Conference on Soil Mechanics and Foundation Engineering, Stockholm, Sweden, Vol. 3, pp. 637-640.
6. Iai, S. and Koizumi, K. (1986). "Estimation of Earthquake Induced Excess Pore Water Pressure for Gravel Drains", Proceedings of the Seventh Japan Earthquake Engineering Symposium, Tokyo, Japan, pp. 679-684.
7. Madhav, M.R. (2001). "Engineering of Ground for Earthquake Disaster Mitigation", Proceedings of the Indian Geotechnical Conference (IGC-2001), Indore, Vol. 2, pp. 29-34.
8. Martin, G.R., Finn, W.D.L. and Seed, H.B. (1975). "Fundamentals of Liquefaction under Cyclic Loading", Journal of the Geotechnical Engineering Division, Proceedings of ASCE, Vol. 101, No. GT5, pp. 423-438.
9. Massarsch, K.R. and Fellenius, B.H. (2002). "Vibratory Compaction of Coarse-Grained Soils", Canadian Geotechnical Journal, Vol. 39, No. 3, pp. 695-709.
10. Murali Krishna, A. (2003). "Liquefaction Mitigation of Loose Sand Deposits by Rammed Granular Piles", MTech Thesis, Indian Institute of Technology Kanpur, Kanpur.
11. Ohbayashi, J., Harda, K. and Yamamoto, M. (1999). "Resistance against Liquefaction of Ground Improved by Sand Compaction Pile Method" in "Earthquake Geotechnical Engineering (edited by P.S. Seco e Pinto)", A.A. Balkema, Rotterdam, The Netherlands.
12. Onoue, A. (1988). "Diagrams Considering Well Resistance for Designing Spacing Ratio of Gravel Drains", Soils and Foundations, Vol. 28, No. 3, pp. 160-168.
13. Pestana, J.M., Hunt, C.E., Goughnour, R.R. and Kammerer, A.M. (1998). "Effect of Storage Capacity on Vertical Drains Performance in Liquefiable Sand Deposits", Proceedings of the Second International Conference on Ground Improvement Techniques, Singapore, pp. 373-380.
14. Seed, H.B. (1979). "Soil Liquefaction and Cyclic Mobility Evaluation for Level Ground during Earthquakes", Journal of the Geotechnical Engineering Division, Proceedings of ASCE, Vol. 105, No. GT2, pp. 201-255.
15. Seed, H.B. and Booker, J.R. (1977). "Stabilization of Potentially Liquefiable Sand Deposits Using Gravel Drains", Journal of the Geotechnical Engineering Division, Proceedings of ASCE, Vol. 103, No. GT7, pp. 757-768.
16. Seed, H.B., Idriss, I.M., Makdisi, F. and Banerjee, N.G. (1975). "Representation of Irregular Stress Time Histories by Equivalent Uniform Stress Series in Liquefaction Analyses", Report UCB/EERC-75/29, Earthquake Engineering Research Center, University of California, Berkeley, U.S.A.
17. Seed, H.B., Lysmer, M.J. and Martin, P.P. (1976). "Pore-Water Pressure Changes during Soil Liquefaction", Journal of the Geotechnical Engineering Division, Proceedings of ASCE, Vol. 102, No. GT4, pp. 323-346.
18. Sujatha, K.P. (1998). "Analysis of Reinforcement and Densification Effects in Improved Ground", MTech Thesis, Indian Institute of Technology Kanpur, Kanpur.
19. Tsukamoto, Y., Ishihara, K., Yamamoto, M., Harada, K. and Yabe, H. (2000). "Soil Densification due to Static Sand Pile Installation for Liquefaction Remediation", Soils and Foundations, Vol. 40, No. 2, pp. 9-20.

20. Yasuda, S., Ishihara, K., Harada, K. and Shinkawa, N. (1996). “Effect of Soil Improvement on Ground Subsidence due to Liquefaction”, Soils and Foundations, Special Issue on Geotechnical Aspects of the January 17, 1995 Hyogoken-Nambu Earthquake, pp. 99-107.